6th European Conference on Computational Mechanics (ECCM 6)
7th European Conference on Computational Fluid Dynamics (ECFD 7)
11 – 15 June 2018, Glasgow, UK

SUPERELASTICITY IN SHAPE MEMORY ALLOYS VIA PERIDYNAMICS

ADAM MARTOWICZ[1]*, JAKUB BRYLA[1], WIESLAW J. STASZEWSKI[1] AND MASSIMO RUZZENE[2,3]

[1]AGH University of Science and Technology, Department of Robotics and Mechatronics,
al. A. Mickiewicza 30, 30-059 Krakow, Poland
e-mail: adam.martowicz@agh.edu.pl, jakbryla@agh.edu.pl,
staszews@agh.edu.pl, url: http://krim.agh.edu.pl/en/

[2]Georgia Institute of Technology, School of Aerospace Engineering,
270 Ferst Drive, GA 30332, Atlanta, USA
[3]Georgia Institute of Technology, School of Mechanical Engineering,
801 Ferst Drive, GA 30332, Atlanta, USA
e-mail: ruzzene@gatech.edu, url: www.ae.gatech.edu

Key words: Peridynamics, Shape Memory Alloys, Superelasticity, Numerical modeling.

Abstract. The work is devoted to modeling the phenomenon of superelasticity, that is present in shape memory alloys (SMA), making use of peridynamics. SMA are a type of smart materials, in which solid phase transformations can be activated either by temperature change or external load. As found in the literature, there are known attempts at simulations of phase transformations in SMA introducing the above-mentioned nonlocal modeling technique. The superelasticity specifically refers to reversible phase changes, i.e. austenite-martensite-austenite, observed in SMA due to cyclic external force loading and unloading. As a consequence, the strain-stress characteristics exhibit hysteretic behavior. However, no temperature variation is needed for superelasticity to initiate phase transformations, as it applies in case of both one- and two-way shape memory effects. Having introduced a peridynamic model for a solid body made of SMA, quasi-static numerical calculations are performed to build a stress-strain characteristics. The reference for the obtained results is provided with the outcomes from finite element analyses. The modelling capabilities of peridynamics for SMA are discussed.

1 INTRODUCTION

Shape memory alloys (SMA), which are considered as a type of smart materials, provide unique and demanded physical properties that allow for many practical applications. In general, the specificity of SMA relates to thermomechanical phenomena present during solid phase transformations. SMA exhibit reversible crystal structure transformations that enable in macro scale [1]: (1) *memorize* one or two geometric shapes respectively via two-way martensitic phase transitions and (2) withstand extraordinary elastic deformation thanks to the phenomenon of superelasticity (also called as pseudoelasticity). In the former case, thermal activation is carried out via heating and cooling an SMA sample. Going through the characteristic material properties, i.e. the temperatures determining when forward and backward martensitic phase transitions begin and finish, one or two different geometric shapes may be achieved by the sample (one- or two-way memory effect). The phase transition processes are spontaneous by their nature. It means that the intermediate shapes of thermally loaded SMA randomly and gradually evolve. However the demanded geometries appear eventually. Hysteretic character of martensitic phase transition is shown in Fig. 1. While temperature variation the contribution of both austenite and martensite phases in the whole body changes.

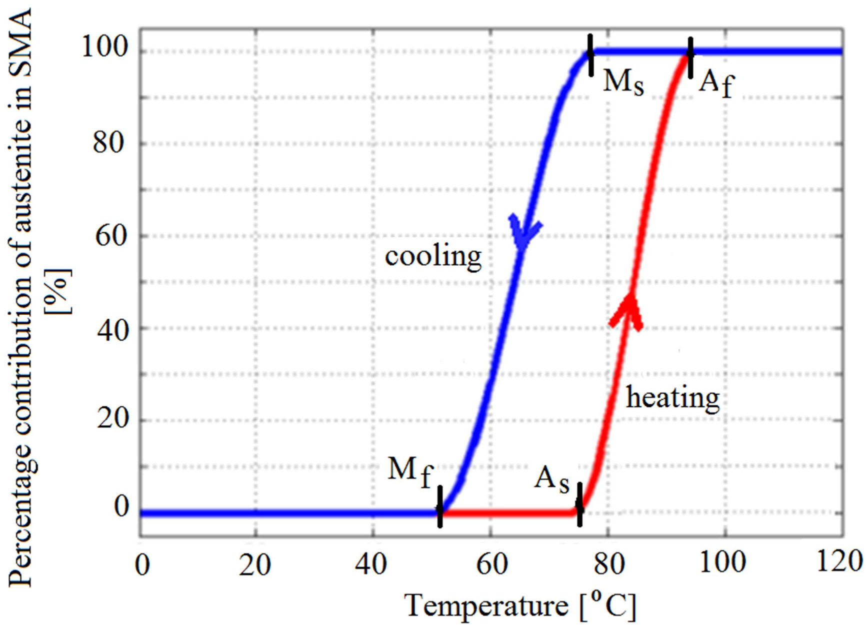

Figure 1: Austenite contribution during reversible phase transition processes activated by the temperature change

As shown in Fig. 1, four characteristic temperatures determine the conditions that have to be satisfied to activate and finish phase transformation processes, in both directions. The two pairs of parameters A_s, A_f and M_s, M_f respectively determine the temperatures when austenite and martensite phases are generated (indexes: *s*-start, *f*-finish). It is worth to be noted that the above mentioned temperatures depend on mechanical stresses – they increase in line with the stress growth. Different shapes of crystal structures for both phases (cubic structure for austenite, rhomboidal structure for martensite) allow for memorizing the geometric shapes while martensitic phase transitions. The case of one-way memory effect is illustrated in Fig 2.

The following repeatable cycle applies for the one-way memory effect: (1) SMA structure deforms while mechanical load at constant temperature – martensite crystals evolve to their deformed variant, (2) stress releases, however, the change of SMA shape is irreversible, (3) memorized shape is recovered while thermal load at zero stress, (4) cooling down leads to the initial state exhibiting undeformed martensite.

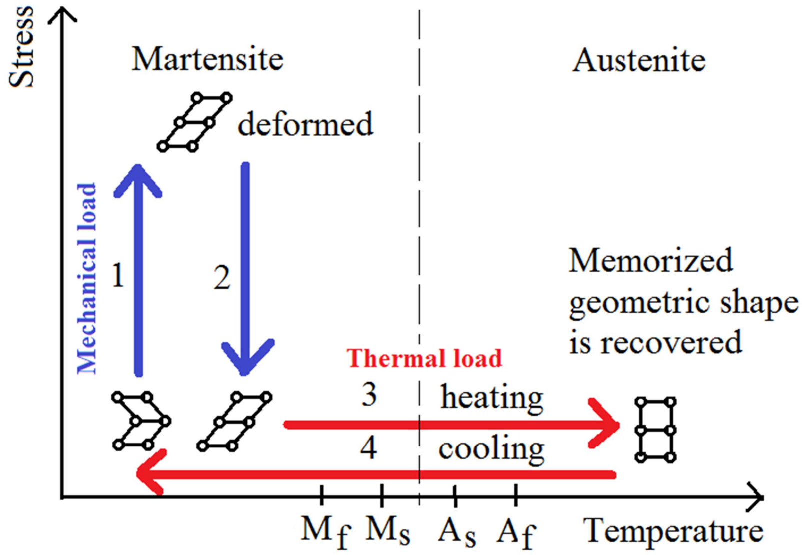

Figure 2: One-way memory effect – application of thermal load is used to recover remembered shape

The latter case of SMA behavior, i.e. superelasticity, reflects the fact that elastic deformations allowed in SMA are considerably high. The maximum strains for SMA exceed 10%, which is much higher that the achievable values for other metallic materials, including copper, steel, aluminum and titanium, which is 1% at most. The phenomenon of superelasticity is explained in more detail in Section 2.

Even though SMA have remained very popular for decades, there is still lack of widely accepted reliable models for this kind of smart materials. Indeed, the number of already published papers on SMA modeling is impressive, which does not solve the issue at all. Overview on the modeling tools can be found in [2]. One reason of the problem is that SMA are still under extensive experimental investigation. Not all phenomena present in SMA are completely studied yet. In consequence, there is still lack of knowledge regarding appropriate modeling techniques that should be used. One of the missing field for SMA that still needs further explanation is the influence of boundary conditions on the material behavior, especially on the course of phase transformation processes [3]. Relatively complicated physics, being still under gradual identification for SMA, requires continuous effort in developing new, more accurate and efficient modeling tools. The above statement reflects the second source of inconveniences during investigation of reliable SMA models, in turn. Based on the formed works described in [4-6] and the model proposed by Lagoudas [7], the authors show in the present paper exemplary results for the approach proposed in [8], which successfully makes use of the theory of peridynamics to model superelasticity [9-11].

The present work consists of 5 sections. After introduction in Section 1, Section 2 provides an overview on the phenomenon of superelasticity, including the Lagoudas analytical model [7]. Next, the peridynamic model for superelasticity in SMA is briefly introduced in Section 3, followed by exemplary application results of the presented approach in Section 4. Section 5 concludes the paper and provides the final conclusions.

2 SUPERELASTICITY IN SMA – ANALYTICAL APPROACH

Superelasticity is observed when force excitation is applied at constant temperature. Austenite should be considered as the initial phase, i.e. the ambient temperature should be greater than A_f. The phenomenon of superelasticity may be explained by the already mentioned fact, that the characteristic temperatures of phase transitions increase while the stress growth, as illustrated in Fig. 3. Hence, purely mechanically imposed phase change (from austenite to martensite – marked with “1” in Fig. 3) allows to withstand significant strains due to both: (1) immediate appearance of deformed versions of rhomboidal structure in created martensite phase, and (2) lower value of elastic modulus (Young’s modulus) for martensite when compared with the respective property of austenite.

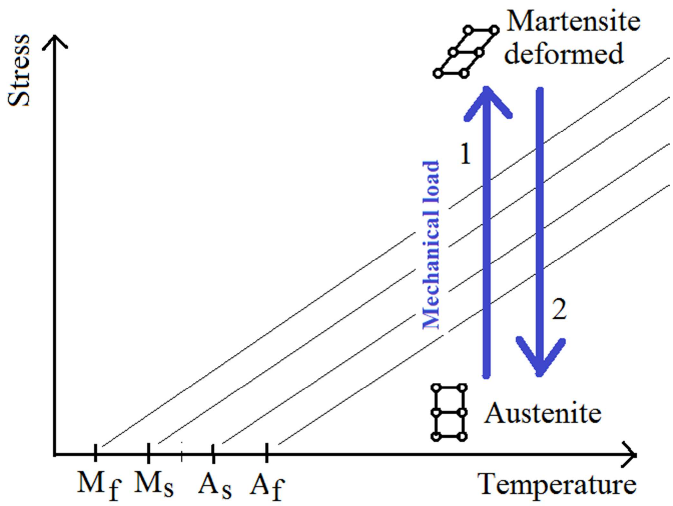

Figure 3: Reversible behavior of SMA for superelasticity – full cycle deals with mechanical loading and unloading an SMA sample.

The effect of superelasticity is reversible. Hence, after external loading is released martensite phase transforms back to austenite instantly. The stress-strain relationship for superelasticity is presented in Fig. 4. As shown, the stress-strain path exhibits hysteresis, which means dependency upon direction of transformation [12]. Moreover, a very interesting region of plateau is present during phase transformation processes – identified for both directions, when the percentage contribution of both phases changes. In this case the stress is kept at almost constant level for a relatively wide range of strain variation. In consequence, a mechanical device generating constant force within the assumed wide range of the stroke may be easily constructed based on SMA.

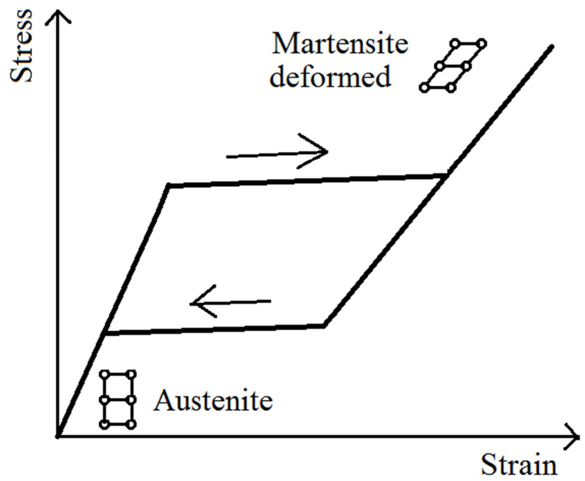

Figure 4: Stress-strain path for superelasticity – full cycle of mechanical loading and unloading an SMA sample.

The unique behavior of SMA (including significant width of the hysteresis loop) allows for applications in damping systems [4,13]. Other commonly known field of application, which makes effective use of superelasticity, is medicine (dental braces and medical staples [14]).

In the following analytical description of the phenomenon of superelasticity is briefly provided. After [7] the total specific Gibbs free energy G, i.e. the total Gibbs free energy per unit mass, for a polycrystalline SMA, constituting a mixture of both austenite and martensite phases, may be calculated with the formula

$$G\left(\bar{\bar{\boldsymbol{\sigma}}}, T, \xi, \bar{\bar{\boldsymbol{\varepsilon}}}^{t}\right) = -\frac{1}{2\rho} C_{ijkl}\sigma_{ij}\sigma_{kl} - \frac{1}{\rho}\sigma_{ij}\left[\alpha_{ij}(T - T_0) + \bar{\bar{\boldsymbol{\varepsilon}}}^{t}\right] + \\ + c\left[(T - T_0) - T\ln\left(\frac{T}{T_0}\right)\right] - s_0 T + u_0 + \frac{1}{\rho} f(\xi) \tag{1}$$

where the arguments of the function G are: $\bar{\bar{\sigma}}$ – second order Cauchy stress tensor, T – temperature, ξ – martensitic volume fraction and $\bar{\bar{\varepsilon}}^{t}$ – second order transformation strain tensor. The quantities σ_{ij} and σ_{kl} stand for a symbolic description of the stress tensor $\bar{\bar{\sigma}}$, following the Einstein summation notation. Hereunder, this notation is used whenever required to unambiguously specify calculations for tensors. The real-valued parameter ξ is taken from the range bounded with the limits: 0 – used to declare pure austenite structure, and 1 if martensite is the only existing phase in the modeled body. Furthermore: ρ – the mass density, C_{ijkl} – fourth order elastic compliance tensor, α_{ij} – second order thermal expansion coefficient tensor, T_0 – reference temperature, c - specific heat, s_0 – specific entropy at a reference state, u_0 – specific internal energy at the reference state, $f(\xi)$ – the transformation hardening function – elastic strain energy originating from the interactions between various variants of martensitic phase and the surrounding phase, including interactions within the martensitic phase.

In case of the considered phenomenon of superelasticity, when temperature effect is not observed (i.e.: $T = T_0$; isothermal phase transformation process initialized by mechanical stresses only), Eq. (1) may be rewritten for a one-dimensional (1-D) case (uniaxial tension) to the form

$$G(\sigma, T, \xi, \varepsilon^t) = -\frac{1}{2\rho} C\sigma^2 - \frac{1}{\rho}\sigma\varepsilon^t - s_0 T_0 + u_0 + \frac{1}{\rho} f(\xi) \tag{2}$$

where the parameter C is defined with reference to the inversions of the Young's moduli for both phases, i.e. E^A and E^M

$$C = C(\xi) = C^A + \xi(C^M - C^A) = C^A + \xi \Delta C, \qquad where: C^A = (E^A)^{-1}, \; C^M = (E^M)^{-1} \tag{3}$$

The indexes A and M denote austenite and martensite phases respectively. All the resultant material parameters used in Eq. (2) are formulated based on the fraction ξ and the properties of the two phases coexisting in the model, similarly to the definition of C with Eq. (3).

The total strain becomes

$$\varepsilon = C(\xi)\sigma + \sqrt{3/2}\, H\xi \tag{4}$$

H is the material property and stands for the maximum uniaxial transformation strain. Having introduced the second law of thermodynamics, to assure that entropy of the modeled body can never decrease, the Clausius-Planck inequality is accordingly formulated based on Eq. (2) in terms of thermodynamic force Π

$$\Pi\dot{\xi} \geq 0 \tag{5}$$

The transformation hardening function $f(\xi)$, may be found using the formula [15]

$$f(\xi) = \begin{cases} \frac{1}{2}\rho b^M \xi^2 + (\mu_1 + \mu_2)\xi, & \dot{\xi} > 0 \\ \frac{1}{2}\rho b^A \xi^2 + (\mu_1 - \mu_2)\xi, & \dot{\xi} < 0 \end{cases} \tag{6}$$

where b^A, b^M, μ_1, μ_2 are the material properties found applying the Kuhn-Tucker conditions

$$b^A = -\Delta s_0 (A_f - A_s) \tag{7}$$

$$b^M = -\Delta s_0 (M_s - M_f) \tag{8}$$

$$\mu_1 = \frac{1}{2}\rho\Delta s_0 (M_s + A_f) - \rho\Delta u_0 \tag{9}$$

$$\mu_2 = \frac{1}{4}\rho\Delta s_0 (A_s - A_f - M_f - M_s) \tag{10}$$

Finally, the thermodynamic force Π takes the form

$$\Pi = \frac{1}{2}\Delta C\sigma^2 + \rho\Delta s_0 T_0 + \Pi_1 \tag{11}$$

$$\text{where } \Pi_1 = \begin{cases} \sqrt{6}H\sigma + \rho\Delta s_0\left(M_s - M_f\right)\xi - \frac{1}{4}\rho\Delta s_0\left(M_s + A_f + A_s - M_f\right), & \dot{\xi} > 0 \\ \sqrt{6}H\sigma + \rho\Delta s_0\left(A_f - A_s\right)\xi - \frac{1}{4}\rho\Delta s_0\left(3M_s + 3A_f - A_s + M_f\right), & \dot{\xi} < 0 \end{cases}$$

Based on the thermodynamic force Π, transformation function Φ is introduced to define conditions when martensitic volume fraction ξ should change

$$\Phi = \begin{cases} \Pi - Y, & \dot{\xi} > 0 \text{ (austenite } \rightarrow \text{ martensite)} \\ -\Pi - Y, & \dot{\xi} < 0 \text{ (martensite } \rightarrow \text{ austenite)} \end{cases} \tag{12}$$

Next, based on the value of Φ, and taking into account the condition (5), two cases apply when change of ξ is required:

- when increasing stress σ, if $\Phi(\dot{\xi} > 0) > 0$, then phase transformation from austenite to martensite is observed and further growth of ξ is required
- when decreasing stress σ, if $\Phi(\dot{\xi} < 0) > 0$, then phase transformation from martensite to austenite is observed and further reduction of ξ is required

The parameter Y is the critical value defying the quantity for internal dissipation while phase transformation

$$Y = \frac{1}{4}\rho\Delta s_0\left(M_s + M_f - A_f - A_s\right) \tag{13}$$

Considering continuously verified conditions regarding transformation function ($\Phi \leq 0$ satisfied at any time) and martensitic volume fraction ($\xi \in [0,1]$) the hysteretic characteristics for superelastic effect (Fig. 4) may be obtained while gradual increase and decrease of the introduced stress.

3 SUPERELASTICITY IN SMA – PERIDYNAMIC MODEL

The governing equation for a peridynamic model of a solid body takes the form [9]

$$\rho u_{,tt} = \int_H f(u' - u, x' - x)dV_{x'} + b \tag{14}$$

where: ρ – mass density, u, u', x, x' - displacements and position respectively for actual central particle and the particle, which is covered by the horizon H, f – pairwise function determining the interactions between particles, b - volumetric density of an external body force, $dV_{x'}$ - portion of volume attached to a neighbouring particle. The function f introduces elastic properties of the modeled body.

For a static 1-D numerical case Eq. (14) takes the following form for the i-the degree of freedom (DOF)

$$\sum_{\substack{j=-N \\ j\neq 0}}^{N} \frac{u_i - u_{i+j}}{|j|} c\beta A + b_i \tag{15}$$

where: j – the index of the neighboring particle, N – determines the horizon ratio (the radius equals NL, where L is the distance between particles, similarly $2N$ – the number of neighboring particles), A – cross-sectional area. The parameter c is the micromodulus function fund based on the geometric and elastic properties

$$c = \frac{2E^A}{(NL)^2 A} \tag{16}$$

and the factor β equals

$$\beta = \begin{cases} 1, j \neq N \wedge j \neq -N \\ \frac{1}{2}, j = N \vee j = -N \end{cases} \tag{17}$$

In case of a uniform rod made of SMA, taking into account Eq. (4) – which is used to determine the total strain in SMA – the following resultant stiffness coefficient may be found [8]

$$k^T = \frac{k}{\alpha_E \xi + 1} \tag{18}$$

where:

$$k = \frac{E^A A}{L} \tag{19}$$

$$\alpha_E = \left(\frac{E^A}{E^M} - 1\right) \tag{20}$$

Similarly, the resultant force is found

$$F^T = \frac{F_M}{\alpha_E \xi + 1} \xi \tag{21}$$

where:

$$F_M = \sqrt{3/2}\, H E^A A \tag{22}$$

Finally, both k^T and F^T are used to formulate the system of linear equations created for all model DOFs based on peridynamic formulation (15). When solving a static or quasistatic problem for subsequent values of the external stretching force, the obtained system of linear equations is appropriately solved to find particle displacements. However, during each simulation step, the conditions regarding the transformation function and martensitic volume fraction, i.e. $\Phi \leq 0$ and $\xi \in [0,1]$ must be checked to assure proper hysteretic behavior of modelled SMA. The next section provides an exemplary results of the peridynamic model of an SMA structure.

4 NUMERICAL CASE STUDY

A simple peridynamic model of a cantilever rod made of 5 particles is considered to confirm capability of the presented approach. The model, which is used to simulate the phenomenon of superelasticity is shown in Fig. 5.

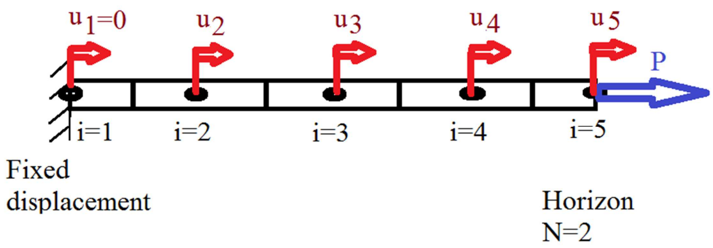

Figure 5: A peridynamic model of an SMA rod used in simulations of the superelasticity effect.

The material properties for SMA were set after [15]. They are collected in Table 1. Cross-sectional area $A = 1mm^2$ whereas the distance between particles $L = 10mm$.

Table 1: Material properties for simulated SMA [15]

Parameter	Value
E^M	30GPa
E^A	70GPa
M_s	291K
M_f	271K
A_s	295K
A_f	315K
$\rho\Delta s_0{}^A$	-0.35MPa/K
$\rho\Delta s_0{}^M$	-0.35MPa/K
H	5%
T_0	473K

The stress-strain paths calculated based on the displacement u_3 for both peridynamic model and referential Finite Element (FE) model are shown in Figure 6.

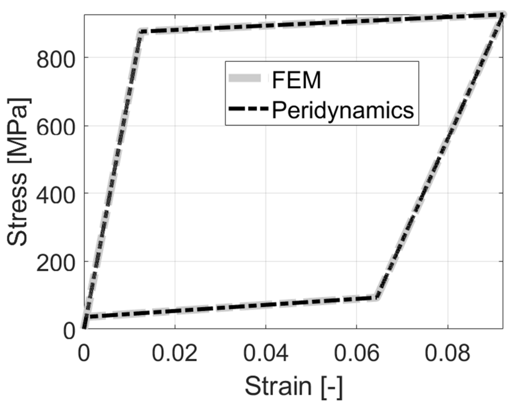

Figure 6: Stress-strain paths observed for the superelasticity effect.

The obtained results for peridynamics and FE method agree. In both cases considered conditions regarding the Clausius-Planck inequality lead to nonlinear material behavior, as demanded. As shown, the proposed implementation of SMA allows for modeling superelasticity effect properly. The external force P changes within sufficiently wide range of values to perform a full cycle for martensitic transition, i.e. the fraction ξ reaches its allowed bounds: 0 (pure austenite) and 1 (pure martensite).

The presented model exhibits wide hysteresis loop that confirms SMA capability of dissipation of considerable amount of energy. The energy dissipated per a cycle corresponds to the area of the drawn hysteresis. This confirms applicability of SMA to dampers.

5 SUMMARY AND CONCLUDING REMARKS

SMA provide unique properties thanks to memory effects and superelasticity. Apart from the already mentioned medical applications, SMA constructions are also successfully applied in aerospace [16]. This fact continuously motivates to improve the quality of models of this type of smart materials. The presented results confirm effectiveness of the approach proposed for modeling superelasticity in SMA. The model makes use of a nonlocally formulated governing equation, i.e. via peridynamics. In contrast to FE method, peridynamics opens new possibilities of modelling material properties, especially in terms of nonlinearities, which applies in case of SMA.

This work has been supported by the AGH University of Science and Technology, WIMiR, research grant no. 11.11.130.560.

REFERENCES

[1] Auricchio, F., Bonetti, E., Scalet, G., and Ubertini, F. Theoretical and numerical modeling of shape memory alloys accounting for multiple phase transformations and martensite reorientation. *International Journal of Plasticity* (2014) **59**:30-54.

[2] Cisse, C., Zaki, W., and Zineb, T.B., A review of modeling techniques for advanced effects in shape memory alloy behavior. *Smart Materials and Structures* (2016) **25**(10): 103001.

[3] Bryła, J., and Martowicz, A., Experimental and numerical assessment of the characteristics describing superelasticity in shape memory alloys – influence of boundary conditions. *ITM Web of Conferences*, (2017) **15**: No. 06007; CMES II - International Conference of Computational Methods in Engineering Science, Lublin, Poland, 23–25 November 2017.

[4] Martowicz, A., Bryła, J., and Uhl, T., *Uncertainty quantification for the properties of a structure made of SMA utilising numerical model.* Proceedings of the Conference on Noise and Vibration Engineering ISMA 2016 & 5th edition of the International Conference on Uncertainly in Structural Dynamics USD 2016, Katholieke University Leuven; Leuven, Belgium, 19–21 September 2016, ID 731.

[5] Bryła J., Palenica, P., and Martowicz, A., *Modeling aspects and simulations for*

properties of shape memory alloys. In: Mańka M. [ed.]: Projektowanie mechatroniczne, zagadnienia wybrane. Akademia Górniczo-Hutnicza, Katedra Robotyki i Mechatroniki, Kraków, (2017): 137–144.

[6] Bryła, J., and Martowicz, A., Shape memory materials as control elements used in a dot Braille actuator. *Mechanics and Control* (in press).

[7] Lagoudas, D.C., Bo, Z.C., and Qidwai, M.A., A Unified Thermodynamic Constitutive Model for SMA and Finite Element Analysis of Active Metal Matrix Composites. *Mechanics of Composite Materials and Structures* (1996) 3:2: 153-179

[8] Martowicz, A., Staszewski, W.J., Ruzzene, M., and Uhl, T., Nonlocal elasticity in shape memory alloys modeled using peridynamics for solving dynamic problems. Nonlinear Dynamics (submitted).

[9] Silling, S.A., Reformulation of elasticity theory for discontinuities and long-range forces. *Journal of the Mechanics and Physics of Solids* (2000) **48**:175–209.

[10] Madenci E., and Oterkus, E., *Peridynamic theory and its applications*. Springer, New York, (2014).

[11] Martowicz A., Peridynamics for damage modelling and propagation via numerical simulations. *Diagnostyka* (2017) **18**(1):73-78.

[12] Lagoudas D., *Shape Memory Alloys: Modeling and Engineering Applications.* Springer, (2008).

[13] Auricchio, F., Fugazza, D., and DesRoches, R., Numerical and experimental evaluation of the damping properties of shape-memory alloys. *Journal of Engineering Materials and Technology* (2006) **128**(3):312-319.

[14] Lecce, L., and Concilio, A., *Shape Memory Alloy Engineering*. Butterworth Heinemann, Chapter 11, (2014).

[15] Lagoudas, D.C., Muhammad, Z.B., Qidwai, A., and Entchev P.B., SMA UM: User Material Subroutine for Thermomechanical Constitutive Model of Shape Memory Alloys. Report, CiteSeerX (2003).

[16] Godard, O., Lagoudas, M., Lagoudas, D., Design of space systems using shape memory alloys. In Proceedings of SPIE, *Smart Structures and Materials*, San Diego, CA, (2003)**5056**:545–558.